Electronic Supplementary Information

for

Characterization of a Heterobimetallic Nonheme Fe(III)-O-Cr(III) Species Formed by O_2 Activation

*Ang Zhou, Scott T. Kleespies, Katherine M. Van Heuvelen and Lawrence Que, Jr.**

Department of Chemistry and Center for Metals in Biocatalysis, University of Minnesota, 207 Pleasant St. SE, Minneapolis, Minnesota 55455, United States

TABLE OF CONTENTS

1. Materials and instrumentation

All reagents and solvents were purchased from commercial sources and used as received unless special noted. The preparation of Fe(TMC)(OTf)$_2$ was carried out following published procedures in nitrogen atmosphere glove box,[1] and iodosylbenzene (PhIO) was synthesized according to published procedures in air.[2]

Elemental analysis was performed by Atlantic Microlab Inc., Norcross, GA, USA. UV/vis spectra were recorded on an HP 8453A diode array spectrometer. Low-temperature visible spectra were obtained using a cryostat from UNISOKU Scientific Instruments, Japan. Electrospray mass spectrometry was performed on a Finnigan LCQ ion trap mass spectrometer. Resonance Raman spectra were collected with 568.2-nm excitation from a Spectra-Physics model 2060 krypton-ion laser and an Acton AM-506 monochromator equipped with a Princeton LN/CCD data collection system. Spectra in Acetonitrile were obtained at 77 K using a 135° backscattering geometry. Samples were frozen onto a gold-plated copper cold finger in thermal contact with a Dewar flask containing liquid N_2. Raman frequencies were calibrated to indene prior to data collection. The monochromator slit width was set for a band pass of 4 cm^{-1} for all spectra. Raman spectral intensities were calibrated relative to the 921-cm^{-1} solvent peak of Acetonitrile. XAS data were collected at beamline X3B at the National Synchrotron Light Source (NSLS) of Brookhaven National Laboratory.

2. Experimental procedures

Synthesis of $Cr(OTf)_2 \cdot 2CH_3CN$ 1.5 g $CrCl_2$ (12.2 mmol) was put in a 50 mL round-bottom flask in nitrogen atmosphere glove box with 10 mL of CH_3CN, and 10 mL of trimethylsilyl trifluoromethanesulfonate (55.3 mmol) was gradually added with vigorous stirring for 8 h, and the solution turned to dark blue. Then vacuum was applied until all the liquid was removed and light blue precipitated was formed. The solid was collected and recrystallized from CH_3CN / $(CH_3CH_2)_2O$, and blue needle crystal was removed from the mother liquor and further dried *in vacuo* (70%). Elemental analysis suggested the final product to be $Cr(OTf)_2 \cdot 2CH_3CN$. Anal. Calcd. for $C6H_6F_6CrN_2O_6S_2$: C, 16.67; H, 1.40; N, 6.48; S, 14.83. Found: C, 16.53; H, 1.60; N, 6.18; S, 14.71.

Titration of $Cr(OTf)_2$ into $[Fe^{IV}O(TMC)](OTf)_2$ 6.1 mg $Fe(TMC)(OTf)_2$ (0.010 mmol) was mixed with 4 mg PhIO (0.018 mol) in 20 mL CH_3CN at r.t. for 30 min, and the 2 mL solution was filtered into a cuvette in UV-Vis instrument at -40 °C. The 0.45 mM concentration of $[Fe^{IV}(O)(TMC)](OTf)_2$ was determined based on its ε value (~ 400 $L\cdot mol^{-1}\cdot cm^{-1}$) at 824 nm. Then 8.0 mg of $Cr(OTf)_2\cdot 2CH_3CN$ was dissolved in 2 mL CH_3CN (1 eq. compared with Fe in 100 uL CH_3CN), and it was titrated into the $[Fe^{IV}(O)(TMC)](OTf)_2$ solution every 25 uL CH_3CN.

XAS data collection. XAS data were collected at beamline X3B at the National Synchrotron Light Source (NSLS) of Brookhaven National Laboratory. Fe K-edge XAS data were collected for frozen solutions maintained at ~30 K over the energy range 6.9-8.0 keV. A Fe foil spectrum was measured simultaneously for internal energy calibration using the first inflection point of the K-edge energy (7112.0 eV). Data were obtained as fluorescence excitation spectra using a solid-state germanium detector (Canberra).

XAS data analysis. Data reduction, averaging, and normalization were performed using the program EXAFSPAK.[3] The coordination number of a given shell was a fixed parameter and was varied iteratively in integer steps while the bond lengths (R) and mean-square deviation (σ^2) were allowed to freely float. The amplitude reduction factor was fixed at 0.9 while the edge-shift parameter E_0 was allowed to float as a single value for all shells. The pre-edge features were fit using the Fityk program[4] with pseudo-Voigt functions composed of 50:50 Gaussian/Lorentzian functions (Fig S4 and Fig S9).

3. Supplementary Information Figures and Tables

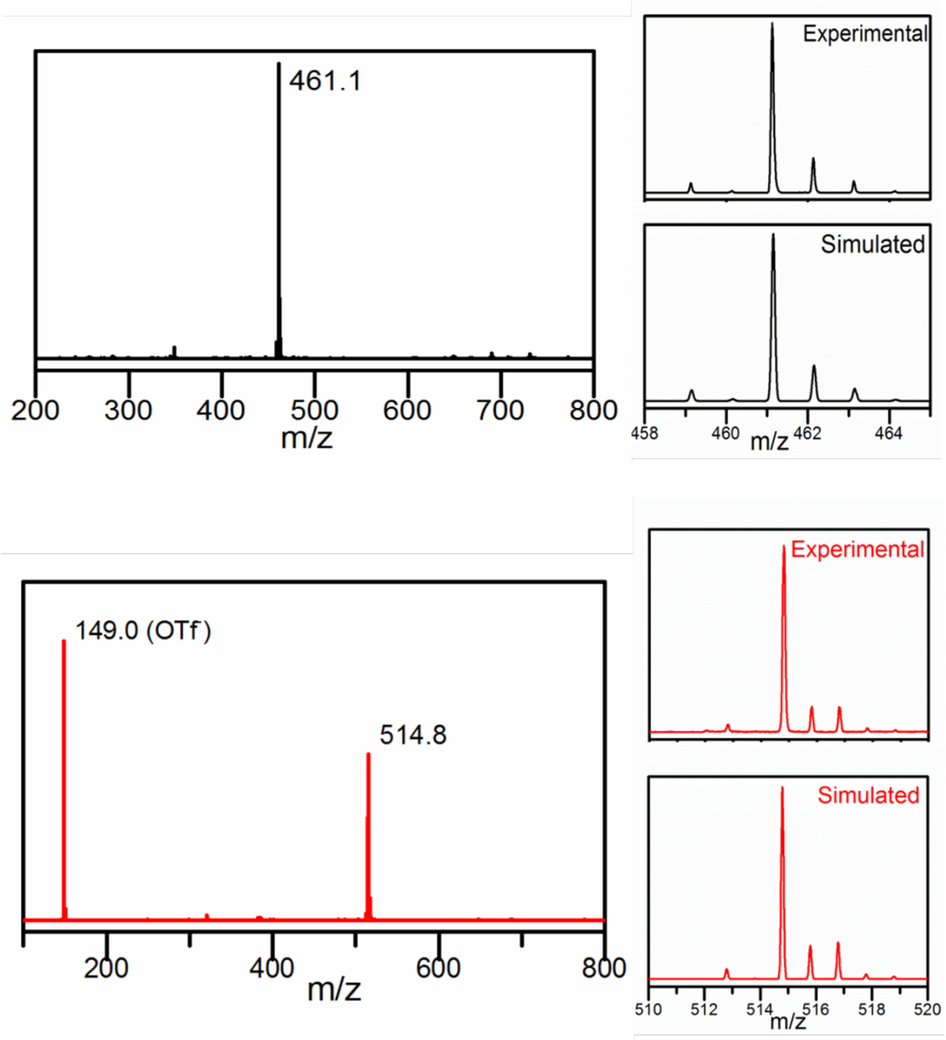

Fig S1 ESI-MS spectra of product from bubbling O_2 into 1 mM $Fe^{II}(TMC)(OTf)_2$ + 1 mM $Cr^{II}(OTf)_2$ solution mixture. Top: positive mode spectrum, together with isotope distribution pattern of the m/z 461.1 peak simulated by $[Fe(TMC)(OTf)]^+$. Bottom: negative mode spectrum, together with isotope distribution pattern of the m/z 514.8 peak simulated by $[Cr(O)(OTf)_3]^-$.

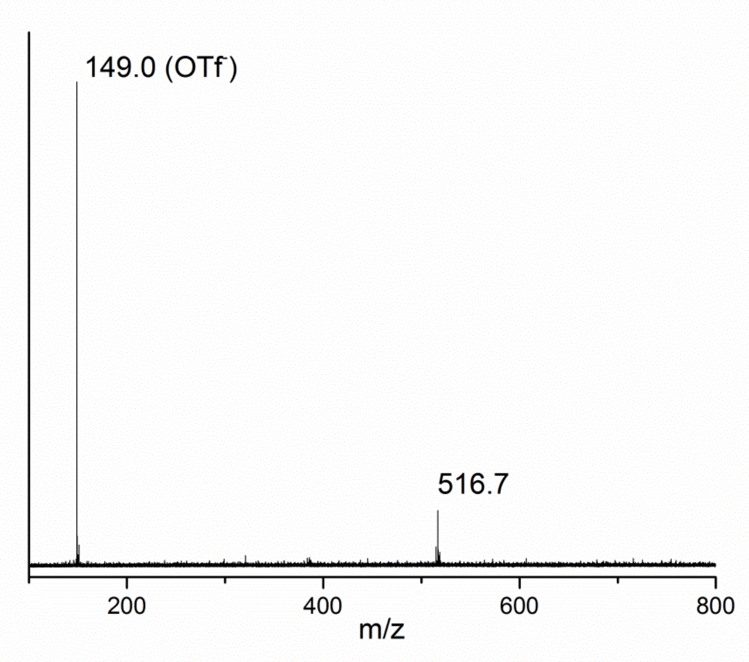

Fig S2 Negative mode ESI-MS spectra of product from $^{18}O_2$ bubbling in 1 mM Fe(II)(TMC)$(OTf)_2$ + 1 mM Cr(II)$(OTf)_2$ solution mixture showing +2 upshift to the m/z 516.7 peak associated with $[Cr(^{18}O)(OTf)_3]^-$.

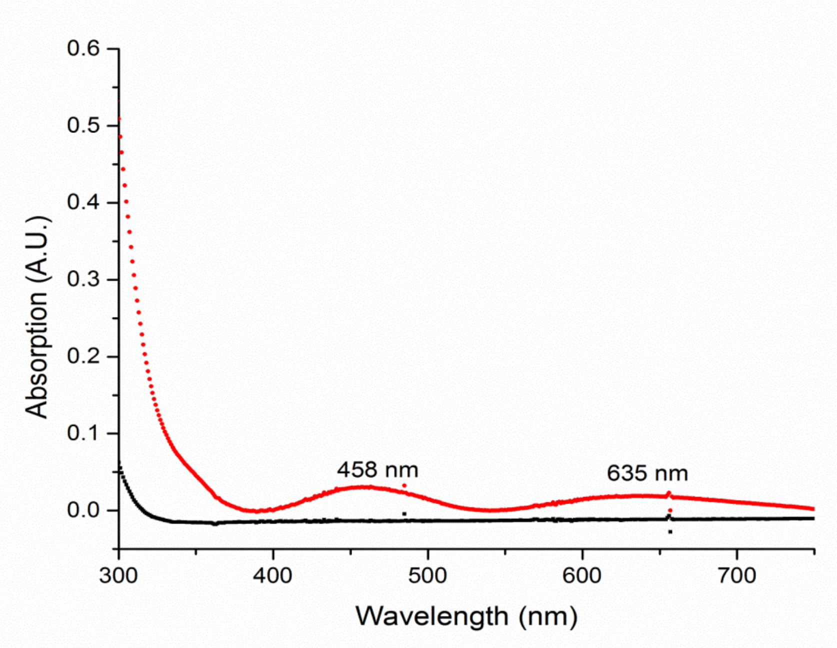

Fig S3 UV-Vis spectra of 1 mM $Cr(OTf)_2$ in CH_3CN before (black) and after addition of 1 eq. PhIO (red).

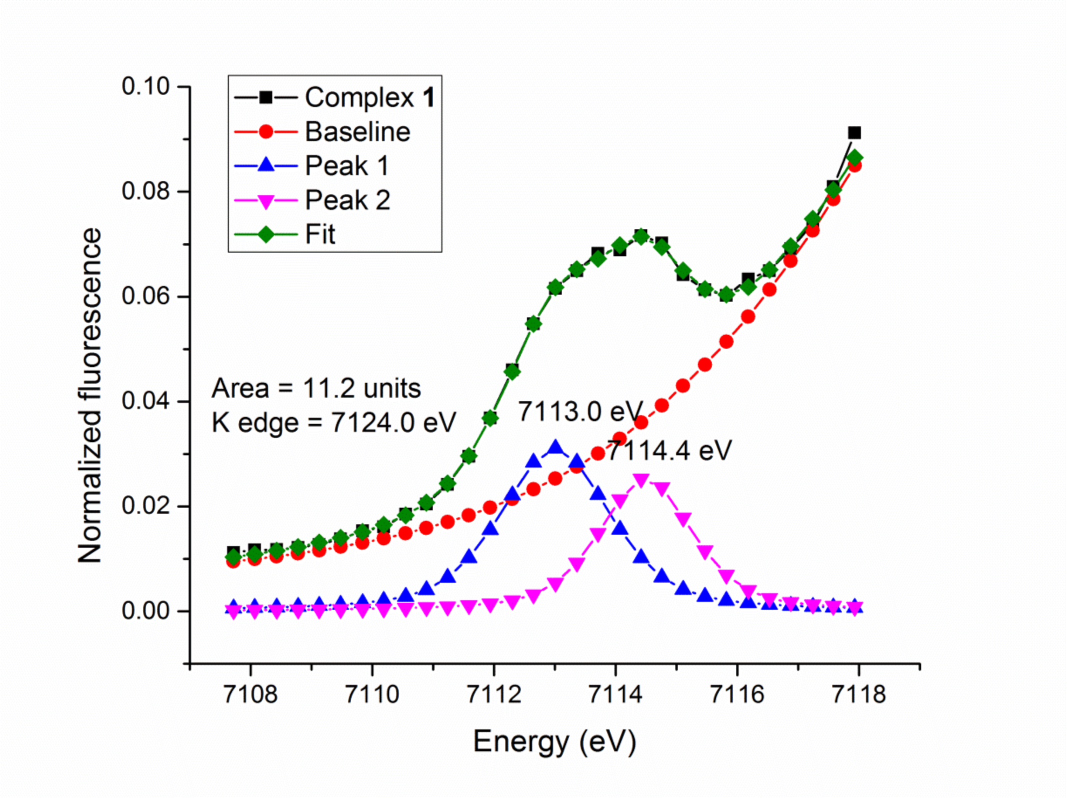

Fig S4 Pre-edge region of Fe K-edge XAS spectrum of **1** (black). Baseline fit (red), pre-edge peak 1 (blue), pre-edge peak 2 (magenta), pre-edge fit (green).

Table S1 Fit parameters for complex **1**. Unfiltered data from 2-12.5 Å^{-1}

	Fe-N/O			Fe-N/O			Fe•••C			Fe•••Cr			E_0	F	F'
Fit	**N**	**R (Å)**	**$\sigma^2 \times 10^{-3}$**	**N**	**R (Å)**	**$\sigma^2 \times 10^{-3}$**	**N**	**R (Å)**	**$\sigma^2 \times 10^{-3}$**	**N**	**R (Å)**	**$\sigma^2 \times 10^{-3}$**			
1	4	2.17	2.10										-9.06	422	591
2	5	2.17	3.47										-8.93	440	604
3	4	2.16	2.47	1	1.82	3.60							-7.85	357	544
4	5	2.16	3.91	1	1.82	2.94							-7.97	337	529
5	5	2.17	3.56	1	1.82	3.50	4	2.90	2.76				-8.72	254	459
6	5	2.16	3.62	1	1.82	3.35	5	2.90	4.62				-8.85	262	466
7	5	2.16	4.04	1	1.81	2.74	4	2.90	6.36	1	3.72	-0.8	-9.48	54	211
8	*5*	*2.17*	*4.12*	*1*	*1.81*	*2.55*	*4*	*2.92*	*6.77*	*1*	*3.65*[a]	*1.00*	*-7.26*	*52*	*207*
9	4	2.17	2.68	1	1.81	3.01	4	2.92	6.42	1	3.65[a]	1.00	-7.19	68	237

[a] Multiple scattering fit

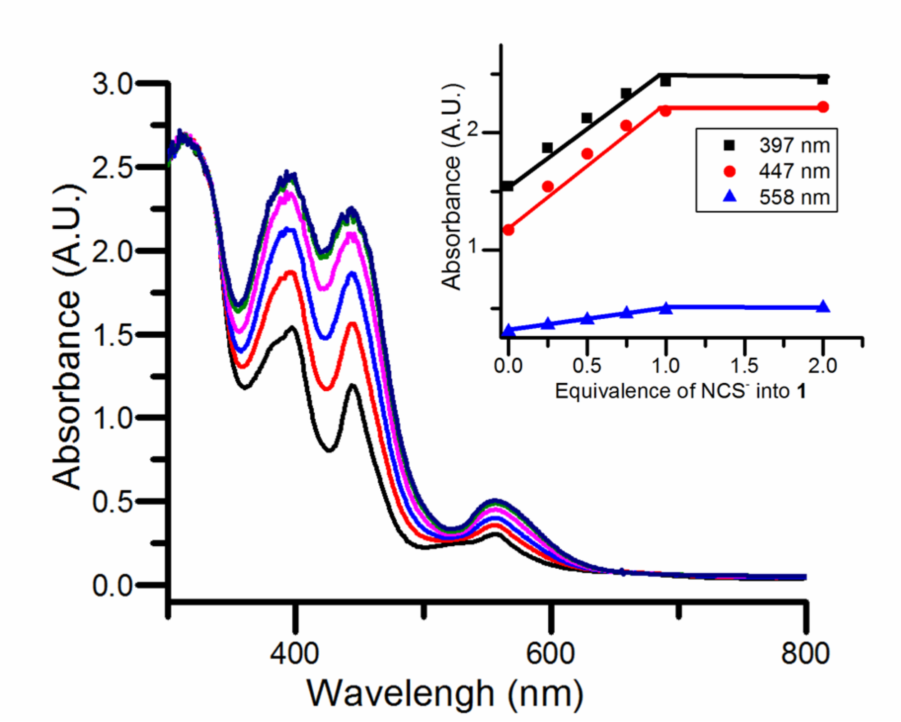

Fig S5 Changes in the UV-vis spectrum of 0.42 mM **1** in CH_3CN upon addition of NBu_4SCN at -40 °C. Black: no NCS^- added. Red: 0.25 eq. of NCS^- added. Blue: 0.5 eq. of NCS^- added. Pink: 0.75 eq. of NCS^- added. Green: 1 eq. of NCS^- added. Purple: 2 eq. of NCS^- added. Inset: Absorbance change as a function of NCS^- equivalents, showing a 1:1 stoichiometry for NCS^- binding to **1**.

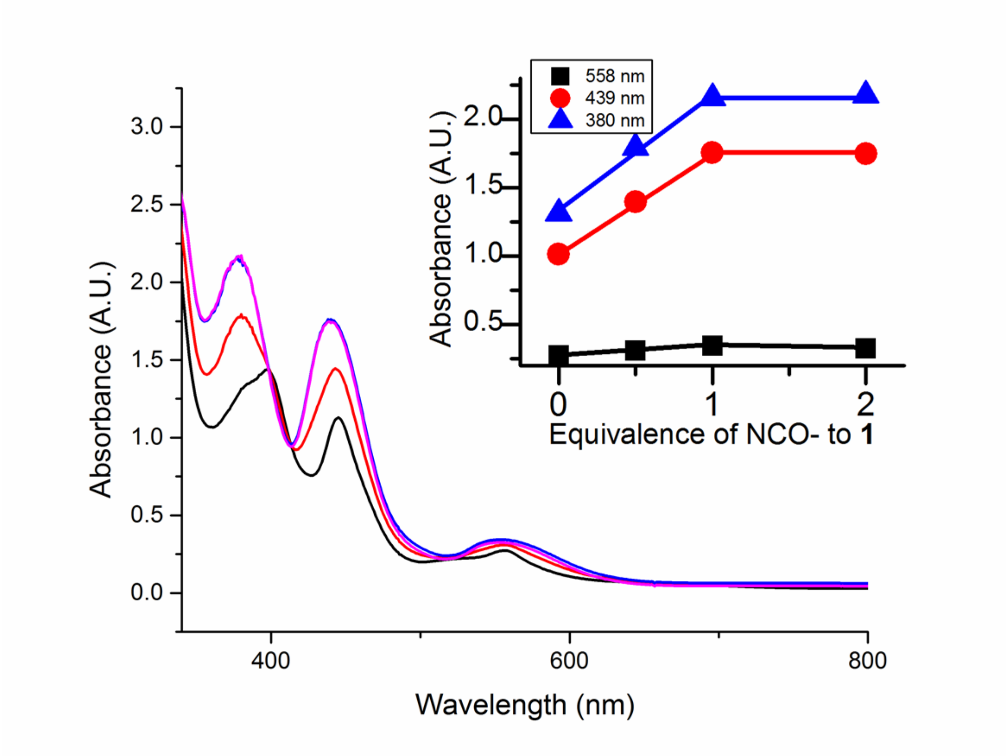

Fig S6 Changes in the UV-vis spectrum when NBu_4NCO was added into 0.4 mM **1** in CH_3CN at -40 °C. Black: no NCO^- added. Red: 0.5 eq. of NCO^- added. Blue: 1.0 eq. of NCO^- added. Pink: 2.0 eq. of NCO^- added. Inset: Absorbance change upon titration of NCO^- into **1**, showing the binding of 1 eq. of NCO^-.

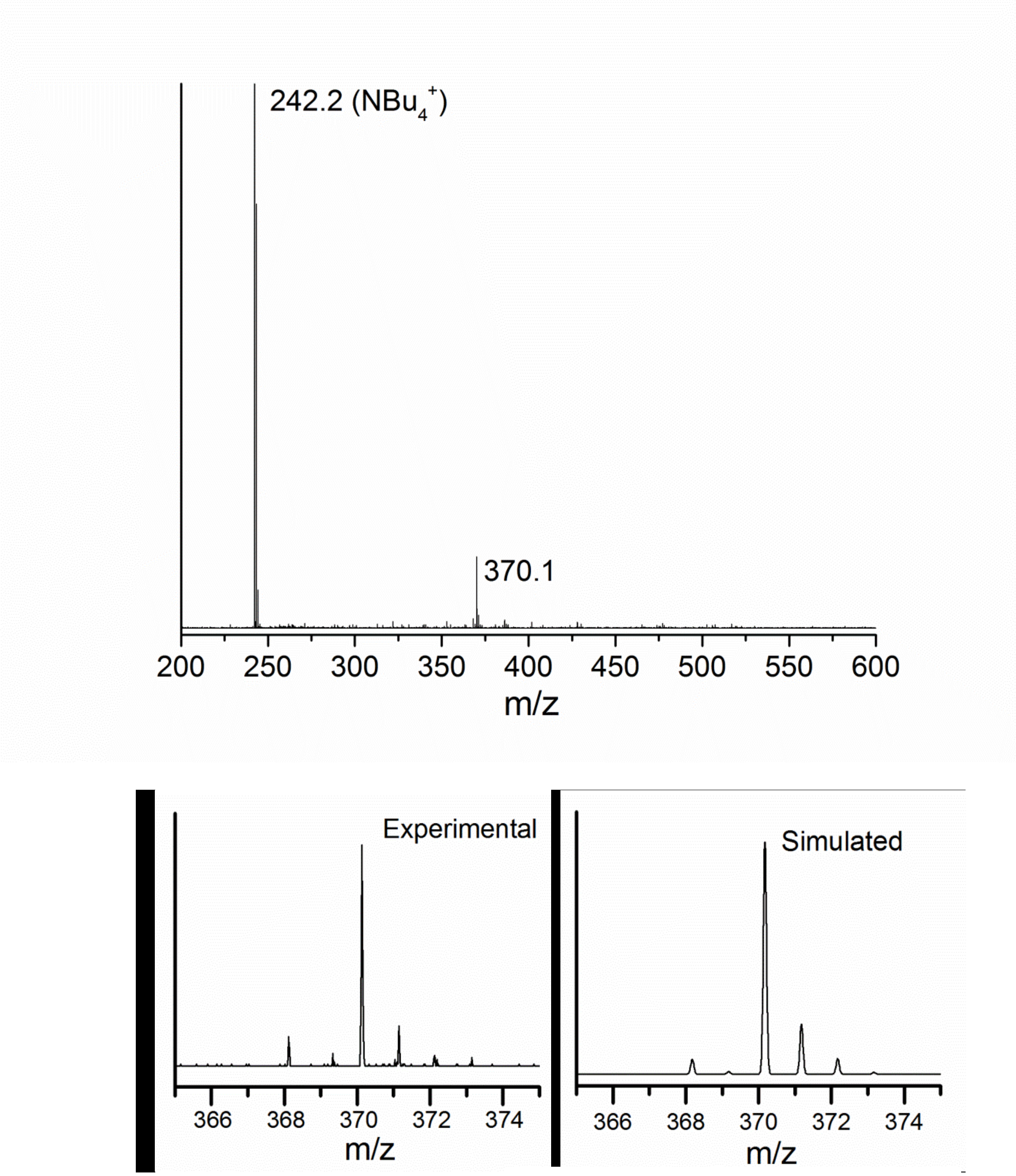

Fig S7 Positive mode ESI-MS spectra observed for the product from 1 mM **1** + 1 eq. NBu_4SCN. The isotope distribution pattern of the m/z 370.1 peak simulated by $[Fe(TMC)(NCS)]^+$.

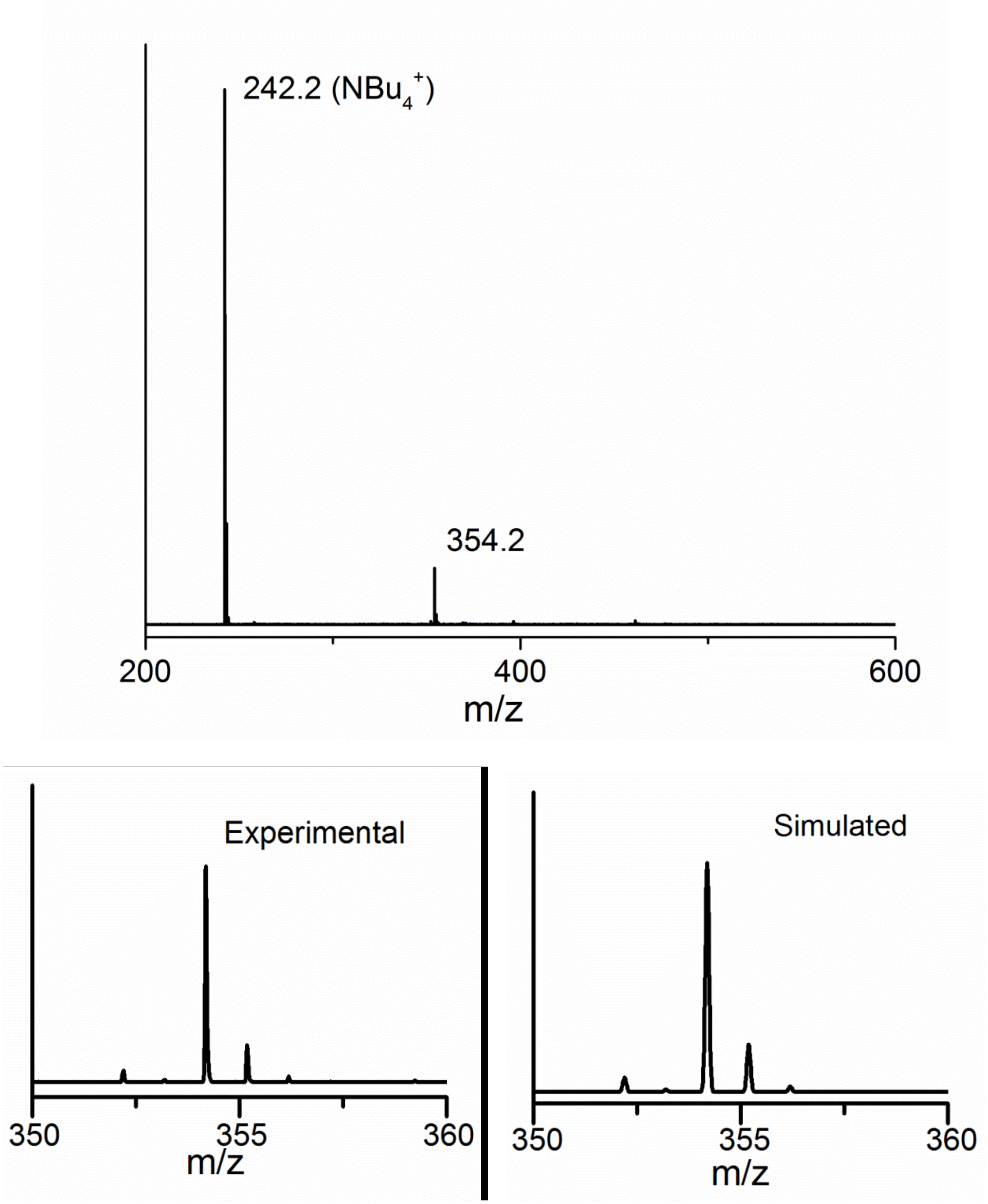

Fig S8 Positive mode ESI-MS spectra observed for the product from 1 mM **1** + 1 eq. NBu_4SCO. The isotope distribution pattern of the m/z 354.2 peak simulated by $[Fe(TMC)(NCO)]^+$.

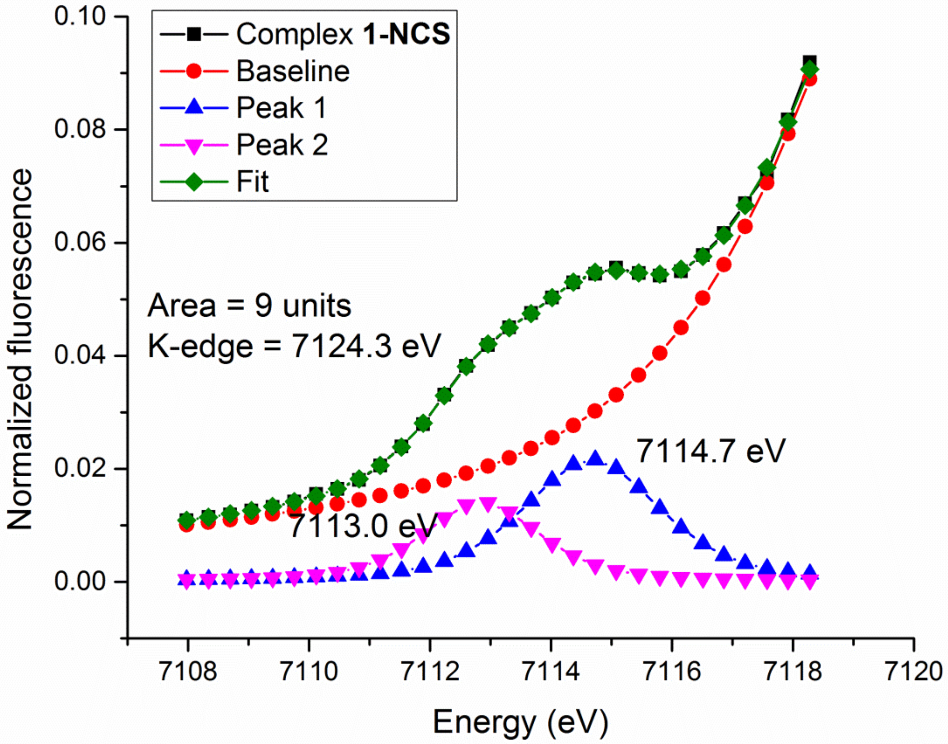

Fig S9 Pre-edge region of Fe K-edge XAS spectrum of **1-NCS** (black). Baseline fit (red), pre-edge peak 1 (blue), pre-edge peak 2 (magenta), pre-edge fit (green).

Table S2 Fit parameters for **1-NCS** unfiltered data from 2-12 Å^{-1}

	Fe-N/O			Fe-N/O			Fe…C			Fe…Cr			E_0	F	F’
Fit	N	R (Å)	$\sigma^2 \times 10^{-3}$	N	R (Å)	$\sigma^2 \times 10^{-3}$	N	R (Å)	$\sigma^2 \times 10^{-3}$	N	R (Å)	$\sigma^2 \times 10^{-3}$			
1	4	2.18	2.0										-4.58	614	672
2	5	2.18	3.6										-4.28	653	693
3	4	2.17	2.7	1	1.85	1.6							-6.44	512	614
4	5	2.17	4.5	1	1.85	0.5							-6.24	489	600
5	5	2.16	4.3	1	1.85	0.7	4	2.90	3.8				-7.34	400	543
6	5	2.16	4.2	1	1.85	1.6	4	2.94	6.9	1	3.75	-0.2	-8.24	139	320
7	*5*	*2.17*	*4.2*	*1*	*1.85*	*1.5*	*4*	*2.95*	*6.4*	*1*	*3.67*[a]	*0.0*	*-6.65*	*76*	*236*
8	4	2.17	2.4	1	1.85	2.9	4	2.96	6.1	1	3.67[a]	0.0	-6.56	84	248

[a] Multiple scattering fit

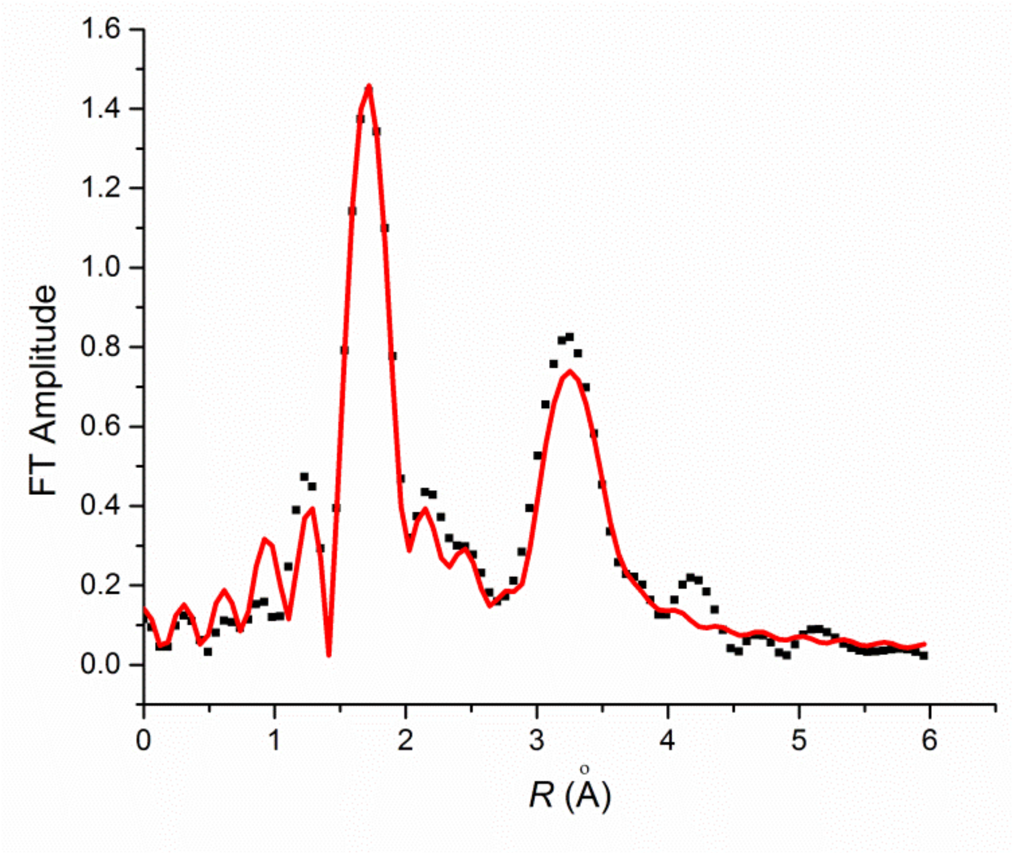

Fig S10 Fit (red line) of the Fourier transformed unfiltered EXAFS data of **1-NCS** (black dots).

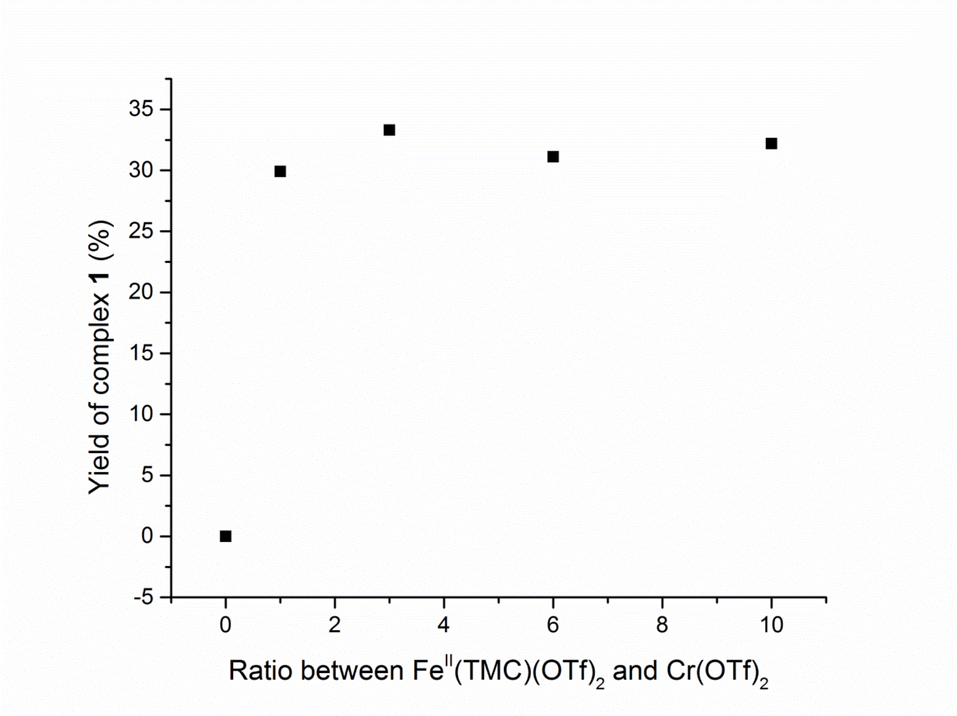

Fig S11 Yields of **1** based on the 558-nm peak intensity upon O_2 bubbling into Fe^{II}(TMC)(OTf)$_2$ + Cr^{II}(OTf)$_2$ solutions in CH_3CN at -40 °C with varying ratios of Fe^{II}(TMC)(OTf)$_2$ to Cr^{II}(OTf)$_2$. Cr^{II}(OTf)$_2$ = 1 mM.

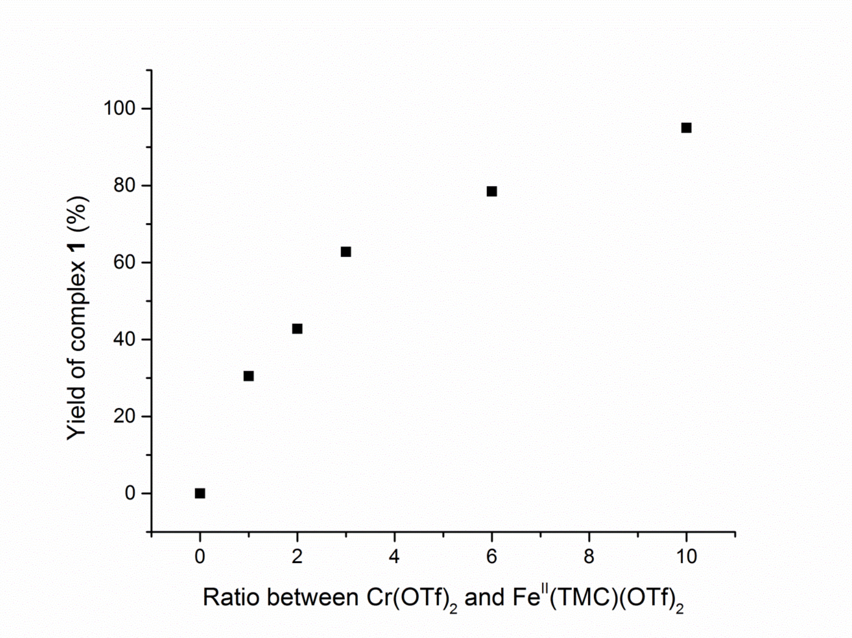

Fig S12 Yields of **1** based on the 558-nm peak intensity upon O_2 bubbling into Fe^{II}(TMC)(OTf)$_2$ + Cr^{II}(OTf)$_2$ solutions in CH_3CN at -40 °C with varying ratios of Cr^{II}(OTf)$_2$ to Fe^{II}(TMC)(OTf)$_2$. Fe^{II}(TMC)(OTf)$_2$ = 1 mM.

4. References

1. J. U. Rohde, J. H. In, M. H. Lim, W. W. Brennessel, M. R. Bukowski, A. Stubna, E. Munck, W. Nam and L. Que, Jr., *Science*, 2003, **299**, 1037-1039.

2. N. Havare and D. A. Plattner, *Org. Lett.*, 2012, **14**, 5078-5081.

3. George, G.N. EXAFSPAK; Standford Synchrotron Radiation Laboratory: Stanford, CA, 1990.

4. FItyk: a general-purpose peak fitting program, Wojdyr, M. *J. Appl. Crystallogr.*, 2010, **43**, 1126-1128.